Novel Stretchable Ambipolar Electrochromic Devices Based on Highly Transparent AgNW/PDMS Hybrid Electrodes

Wei-Hao Chen, Fang-Wei Li, and Guey-Sheng Liou*

Novel stretchable ambipolar electrochromic devices (ECDs) based on highly transparent silver nanowire (AgNW)/polydimethylsiloxane (PDMS) hybrid electrodes are successfully prepared in this study. A facile fabrication methodology has been proposed for the preparation of highly transparent and stretchable ECDs by judiciously combining electrochromic materials and AgNW/PDMS hybrid electrodes. Additionally, these stretchable ECDs are composed of an ambipolar system based on triphenylamine derivatives and heptyl viologen. The obtained stretchable ECDs based on the AgNW/PDMS hybrid electrodes are initially colorless; these ECDs exhibit high transparency at the neutral state and reveal various colors according to different ambipolar redox couples at the related applied potentials.

1. Introduction

Electronic devices with flexible or even stretchable characteristics are commercially attractive in the coming generation. Metallic oxides such as indium tin oxide (ITO) and fluorine-doped tin oxide (FTO), have occupied a dominant position in the market place because of their outstanding properties in both electrical and optical performance. However, the drawbacks in terms of brittleness and high cost are critical restrictions for further development. Therefore, some feasible materials including carbon nanotubes (CNTs),[1,2] graphenes,[3] and metallic nanowires have attracted immense attention due to their flexibility. Among these conductive nanomaterials, 1D metallic nanowires especially silver nanowires (AgNWs) and carbon nanotubes (CNTs), exhibit excellent transmittance and flexibility, which have been considered as the best potential candidates for transparent conductive electrodes (TCEs). Nevertheless, CNT-polymers still face some critical challenges for developing colorless and highly transparent conductive films (TCFs) that possess superior optoelectronic properties and excellent mechanical flexibility by utilizing continuous large-scale preparation. These

challenges can be ascribed to the following crucial issues: a) inhomogeneous dispersion of high-quality CNTs in solvent; b) the lack of a continuous large-scale fabrication method for CNT-polymer TCFs; c) the complex and costly fabrication process for obtaining CNTs with high purity.[2] In 2002, Xia's group found that AgNW could be readily prepared on a large scale,[4] thus solving the problems associated with CNT-polymer TCFs.

With the development of science and technology, polymer nanocomposites are widely used in versatile applications owing to their tunable properties, such as electromagnetic interference (EMI) shielding,[5] multifunctional coatings,[6] environment remediation,[7] and electronic devices.[8] Moreover, substrates, such as polyethylene terephthalate (PET), polyvinyl alcohol (PVA), and polydimethylsiloxane (PDMS), for device fabrication have been widely used for incorporation with AgNWs.[8] Among them, PDMS not only shows strong adhesion to AgNWs but also exhibits excellent stretchability with higher toughness and flexibility than other flexible substrates. Through the combination of AgNWs and flexible substrates, highly transparent and flexible/stretchable hybrid electrodes could be easily obtained for next-generation optoelectronics.

Electrochromism is a mechanism by which some materials can exhibit reversible color conversions caused by changing their optical absorption characteristics during electrochemical reduction or oxidation processes. Numerous representative electrochromic (EC) materials have been reported, such as transition metal oxides like tungsten trioxide (WO_3),[9] inorganic coordinating complexes of Prussian blue[10] and terpyridine complexes,[11] conjugated polymers,[12] and organic molecules including viologen,[13] and triphenylamine (TPA) derivatives. Our group has been working on the development of TPA-containing EC materials, including TPA derivatives and TPA-based high-performance polymers,[14] for quite a long time. These materials generally are highly transparent and colorless at the neutral state and reveal obviously polyelectrochromic coloring behaviors during electrochemical oxidation. In our latest publication, panchromatic electrochromic devices (ECDs) were also successfully fabricated by using an ambipolar system of TPA derivatives and heptyl viologen (HV); the obtained devices could switch from a highly transparent and colorless neutral form to a truly black oxidized state.[15]
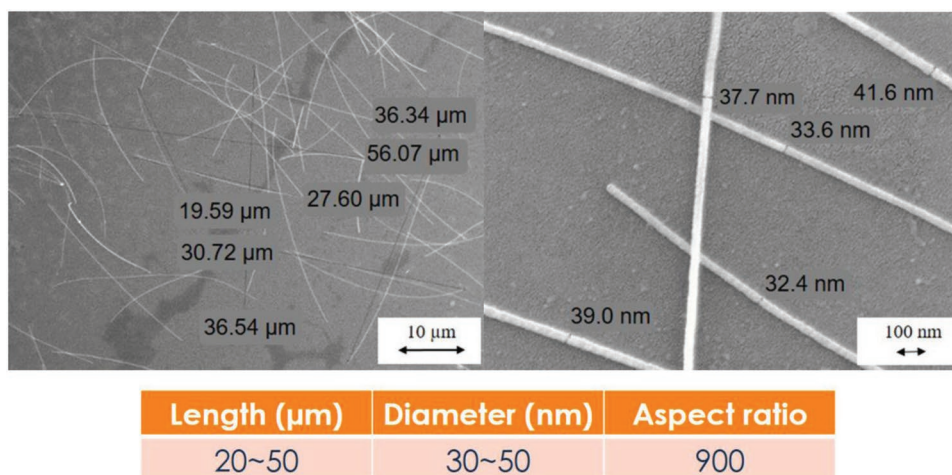
However, most conventional ECDs exhibit their attractive properties on ITO-coated substrates. With the progress of science and technology, the development of stretchable and transparent materials as substrates has become more feasible, and interesting results concerning flexible EC systems based

W.-H. Chen, F.-W. Li, Prof. G.-S. Liou
Institute of Polymer Science and Engineering
National Taiwan University
1 Roosevelt Road, 4th Sec., Taipei 10617, Taiwan
E-mail: gsliou@ntu.edu.tw
Prof. G.-S. Liou
Advanced Research Center for Green Materials Science and Technology
National Taiwan University
Taipei 10617, Taiwan

The ORCID identification number(s) for the author(s) of this article can be found under https://doi.org/10.1002/adom.201900632.

ADVANCED
SCIENCE NEWS

www.advancedsciencenews.com

ADVANCED
OPTICAL
MATERIALS

www.advopticalmat.de

Length (µm)	Diameter (nm)	Aspect ratio
20~50	30~50	900

Figure 1. Scanning electron microscopy images of the prepared AgNWs coated on the glass substrate.

on AgNWs and WO₃ have been reported.[16] In addition, AgNW-based stretchable ECDs have been developed very recently.[17] Although these ECDs have present excellent results with regard to stretch capability and EC performance, the lack of diversity in EC color changes in these examples is still a critical issue.

Herein, we tried to increase the diversity in color changes of stretchable ECDs by introducing an ambipolar EC system based on a series of TPA derivatives and heptyl viologen (HV) into AgNW/polydimethylsiloxane (PDMS) hybrid electrodes for the first time. Subsequently, EC behaviors of the obtained stretchable devices were systematically investigated in this work for future optoelectronic applications.
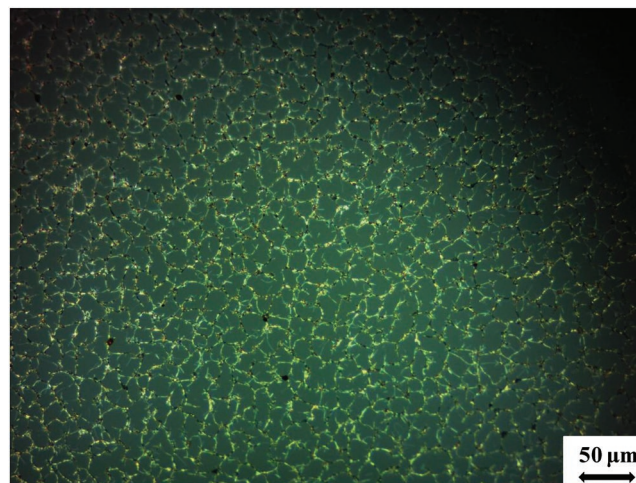
2. Results and Discussion

2.1. Basic Characterization of High Aspect Ratio AgNW

The transparency of AgNW-based electrodes is extremely influenced by aspect ratio of the obtained AgNWs. To achieve better performance for stretchable electrodes, an AgNW sample with a high aspect ratio was prepared by the modified procedures of a previous studies utilizing NaCl and KBr as conucleating agents.[8a] A high aspect ratio of approximately 900 of AgNWs with 35 µm as the average length and a 40 nm average diameter could be successfully obtained as confirmed by the scanning electron microscopy (SEM) images shown in **Figure 1**.
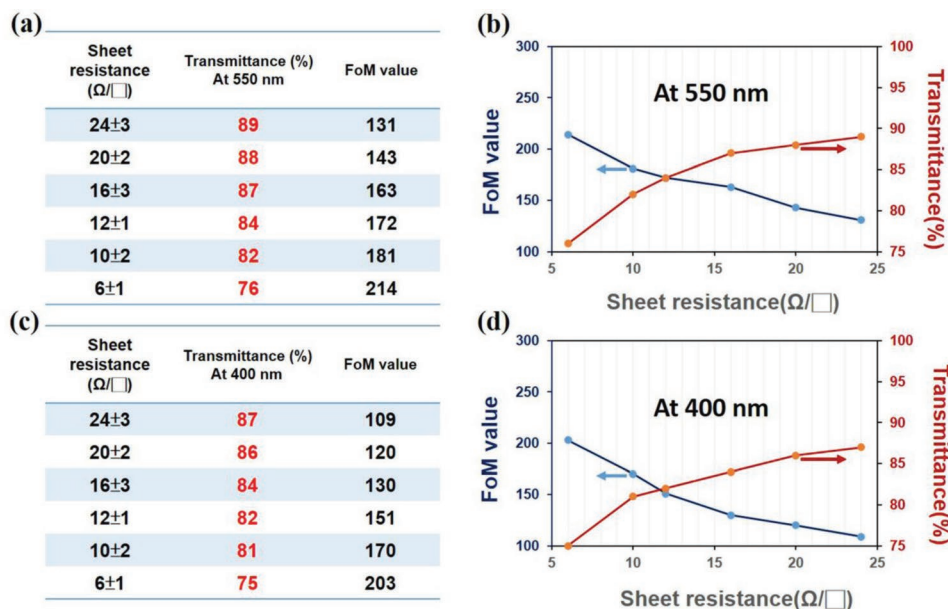
2.2. Properties of AgNW/PDMS Hybrid Electrodes

The optical microscope (OM) image of as-sprayed AgNW/PDMS electrodes shown in **Figure 2** demonstrates that the AgNW network could be uniformly distributed throughout the surface of the PDMS substrate. This result can be ascribed to the three main conditions of spraying techniques. First, PDMS was preheated at 120 °C on a hotplate before being sprayed to evaporate ethanol immediately during the spraying AgNW process to overcome the incompatibility between hydrophobic PDMS and hydrophilic ethanol and to avoid creating an opaque

surface from the aggregation of AgNW/ethanol solution. Second, AgNWs were spray-coated onto the PDMS substrate with an interval of one second, and this step could introduce an appropriate amount of AgNWs to have an immediate and real impact on transmittance. Third, AgNW/ethanol solution with high back pressure of 20 psig was used to generate stronger shear force at the nozzle for spraying out smaller droplets.[18] Shrinking the size of the droplets could efficiently enhance the transparency of the AgNW/PDMS hybrid electrodes because these smaller droplets would more easily evaporate and prevent nonuniformity in the AgNW percolation network. Consequently, controlling these important parameters in every step could give rise to better optical properties. The electrical and optical properties of these stretchable and transparent AgNW/PDMS electrodes are illustrated in **Figure 3**. Because of the nanoscale diameter of the metal wires, visible light could easily pass through the AgNW networks, resulting in the high transparency of these hybrid electrodes. Along with the higher contents of AgNWs on PDMS, the sheet resistance and transparency of the hybrid electrodes decreased simultaneously, as depicted in Figure 3, displaying an optical transmittance (air as

Figure 2. Optical microscopy image of the AgNW/PDMS hybrid electrode.

ADVANCED
SCIENCE NEWS
www.advancedsciencenews.com

ADVANCED
OPTICAL
MATERIALS
www.advopticalmat.de

(a)

Sheet resistance ($\Omega/\square$)	Transmittance (%) At 550 nm	FoM value
24±3	89	131
20±2	88	143
16±3	87	163
12±1	84	172
10±2	82	181
6±1	76	214

(c)

Sheet resistance ($\Omega/\square$)	Transmittance (%) At 400 nm	FoM value
24±3	87	109
20±2	86	120
16±3	84	130
12±1	82	151
10±2	81	170
6±1	75	203

Figure 3. The characteristics of AgNW/PDMS hybrid electrodes without binder at different wavelengths: a), b) at 550 nm and c), d) at 400 nm (based on air as the background).

background) at a higher value of approximately 75% with sheet resistance of 6 Ω sq^{-1}.

To improve the weak adhesion between AgNWs and the PDMS substrate, a thin layer of PDMS as a binder was spin-coated onto the surface of the substrate, which could effectively prevent the AgNW network from peeling off of the PDMS substrate. Since the binder layer was very thin, the inclusion of PDMS only increased sheet resistance by 1 to 2 Ω sq^{-1} without sacrificing the transmittance of the electrodes after spin-coating. In the published literature, spin-coating PDMS/chloroform solution (50 mg per 1 mL) onto AgNW/PET hybrid electrodes could efficiently obtain a protection layer.[19] However, this condition was not suitable in our case of replacing the PET substrate by PDMS. After many attempts, we found that PDMS/hexane as the spin-coating solution could achieve optimal optical performance due to the excellent compatibility of hexane and PDMS, which leads to the best wettability. The resulting AgNW/PDMS hybrid electrodes are also shown in **Figure 4** for comparison of the optical transparency with ITO-coated glass. The figure of merit (FoM) value could be surpassed owing to lower sheet resistance as depicted in Figure 3b, while the transparency is also an important parameter for the requirement of ECDs. Consequently, the AgNW/PDMS hybrid electrode with 87% transmittance and sheet resistance of 16 Ω sq^{-1} was chosen for the ECD fabrication and further investigation of the optoelectronic behaviors.

2.3. Electrochromic Behaviors of ECDs Based on AgNW/PDMS Hybrid Electrodes

In this section, brittle ITO-coated glass was replaced by stretchable AgNW/PDMS electrodes. Before applying stretchable AgNW/PDMS electrodes to the fabrication of ECD, the brittle
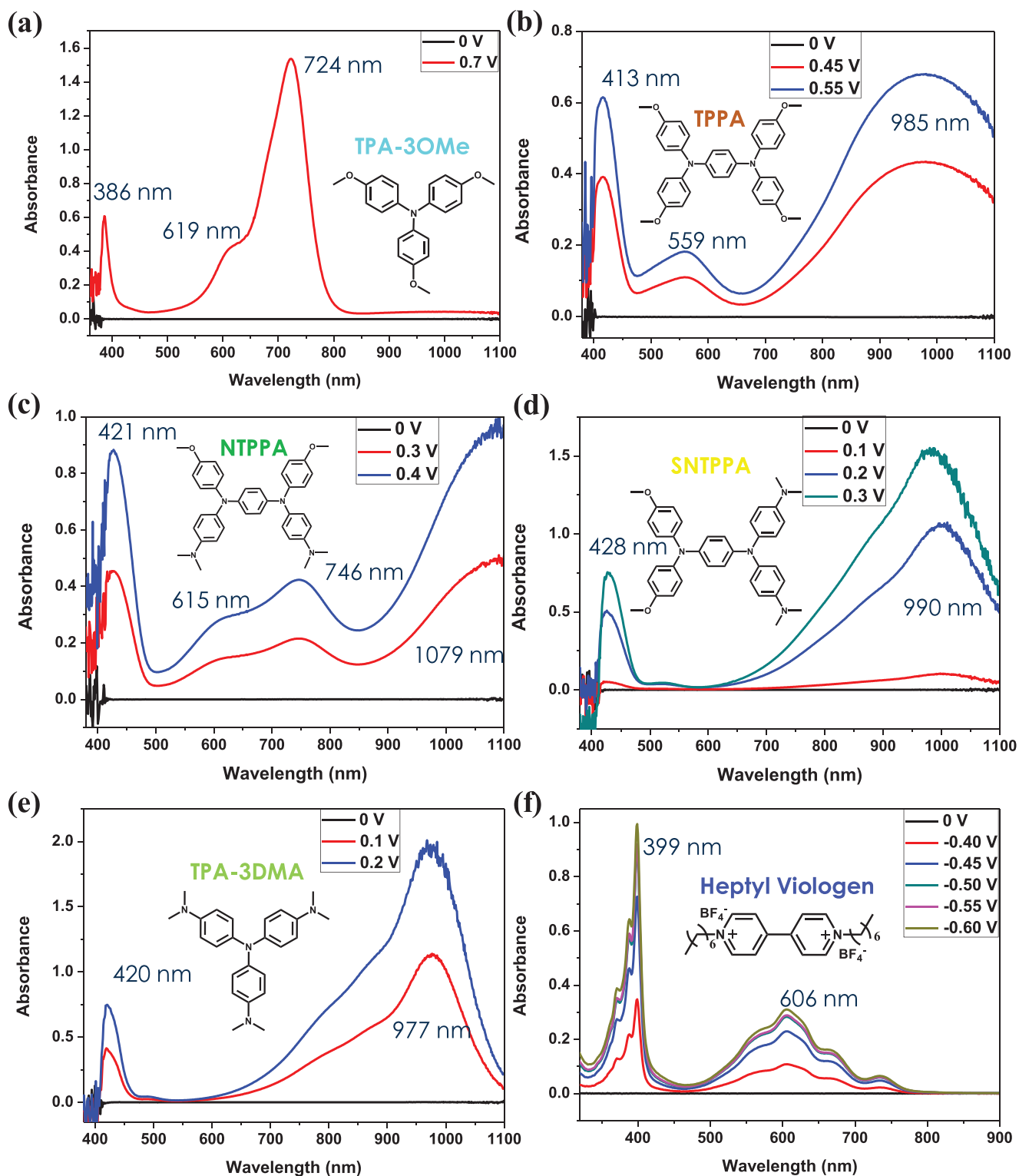
ITO-coated glass was first replaced by stretchable AgNW/PDMS electrodes to study the intrinsic electrochemical and EC behaviors of these EC materials which were measured by cyclic voltammetry (CV) using a three-electrode system with Pt wire and Ag/AgCl as the counter and reference electrode, respectively, in 0.5 M TBABF$_4$ electrolyte.

The electrochemical and EC behaviors of **TPA-3OMe** were first measured on the AgNW/PDMS hybrid electrodes. According to a previous study,[20] the first oxidation state of **TPA-3OMe** should appear at 0.6 V (versus Ag/AgCl) with a color change from colorless to sky-blue. The CV diagram of **TPA-3OMe** in propylene carbonate (PC) solution with TBABF$_4$ as electrolyte by using AgNW/PDMS as the working electrode is presented in Figure S1a, Supporting Information, which
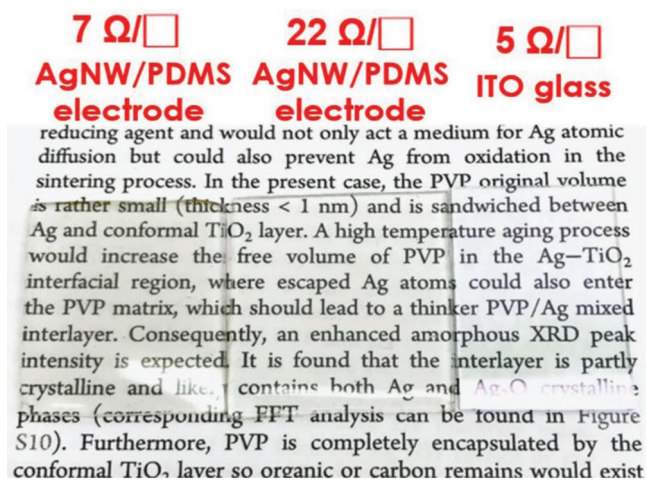
Figure 4. Comparison of transparency between AgNW/PDMS hybrid electrodes and ITO-coated glass with different sheet resistances.
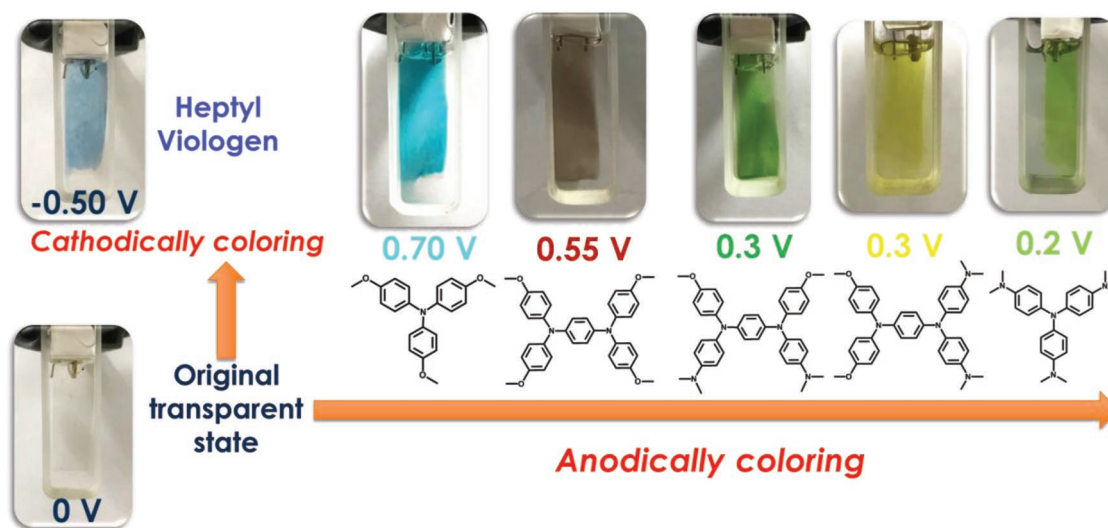
1900632 (3 of 9)

ADVANCED
SCIENCE NEWS
www.advancedsciencenews.com

ADVANCED
OPTICAL
MATERIALS
www.advopticalmat.de

Figure 5. Absorption spectra of different electrochromic materials: 0.017 mmole of a) **TPA-3OMe,** b) **TPPA,** c) **NTPPA,** d) **SNTPPA,** e) **TPA-3DMA,** f) **HV,** and 0.068 mmole TBABF$_4$ in 2.8 mL propylene carbonate at different applied potential. (AgNW/PDMS hybrid electrodes served as the working electrodes at 1 cm thick for the OTTLE cell).

reveals that with the current increasing in sync with oxidation, **TPA-3OMe** starts to change color at 0.6 V (versus Ag/AgCl). In addition, from the UV–vis spectrum of **TPA-3OMe** shown

in **Figure 5**a, new absorption peaks at 386, 619, and 724 nm appear, indicating that **TPA-3OMe** was oxidized and adsorbed onto the AgNW/PDMS hybrid electrode at an applied potential

ADVANCED
SCIENCE NEWS
www.advancedsciencenews.com

ADVANCED
OPTICAL
MATERIALS
www.advopticalmat.de

Figure 6. Summary of EC diversity in color changes with the stretchable AgNW/PDMS hybrid electrodes serving as the working electrode.

of 0.7 V (versus Ag/AgCl) and demonstrating the same color changes from colorless to sky-blue color that is depicted in **Figure 6**. These results are also highly consistent with the published literature for studies using ITO-coated glass as the working electrode.[20]

In our previous report,[15] the oxidation potential of **TPPA** was actually lower than **TPA-3OMe** because of the higher electron density at the redox-active nitrogen atoms, and the material could change colors from colorless to brown at 0.5 V (versus Ag/AgCl). Thus, the oxidation onset of **TPPA** at 0.4 V (versus Ag/AgCl) could be observed in the electrochemical test by using AgNW/PDMS as the working electrode, as shown in Figure S1b, Supporting Information. The light absorption characteristics of **TPPA** during the electrochemical process presented in Figure 5b display three absorption peaks at 413, 559, and 985 nm with color changes from colorless to brown for an applied potential set at 0.45 V (versus Ag/AgCl) as depicted in Figure 6. The absorption peak in the near-IR region could be classified as the intervalence charge transfer (IV-CT) excitation, associated with the electron transfer from the active neutral nitrogen atom to the cation radial nitrogen center through the bridge of the phenyl ring.

The third EC material, **NTPPA**, was designed via replacing two methoxy substituents on both sides of **TPPA** by dimethylamino groups. Interestingly, **NTPPA** exhibits a lower first oxidation potential than the structurally similar **TPPA** due to the stronger electron-donating capability of the dimethylamino moiety. In addition, the EC behaviors are obviously different for **TPPA** and **NTPPA** at their first oxidation state. As depicted in Figure S1c, Supporting Information, the oxidation process of **NTPPA** started at 0.2 V (versus Ag/AgCl), meanwhile; the UV-Vis absorption spectrum of **NTPPA** presented in Figure 5c exhibits four absorption peaks located at 421, 615, 746, and 1079 nm with a color change from colorless to green (Figure 6) for an applied potential set at 0.3 V (versus Ag/AgCl) related to the first oxidation state.

Furthermore, a new compound, **SNTPPA**, as described in supporting information, was also synthesized to expand the EC

diversity in color with AgNW/PDMS hybrid electrodes, and to compare the EC characteristics with isomeric **NTPPA** having different positions of methoxy and dimethylamino substituents. The onset of oxidation for **SNTPPA** at 0.15 V (versus Ag/AgCl) could be observed from the CV diagram presented in Figure S1d, Supporting Information, and the UV–vis optical absorption spectrum of **SNTPPA** during the electrochemical process illustrated in Figure 5d reveals two absorption peaks at 428 and 990 nm; a color change from colorless to yellow was observed when the applied potential was set at 0.2 V (versus Ag/AgCl). Surprisingly, even though **NTPPA** and **SNTPPA** are isomers, their changes in color are converse at their corresponding first oxidation state as shown in Figure 6. To evaluate more EC color changes that could be introduced into AgNW/PDMS ECDs, **TPA-3DMA** was also prepared and incorporated into the AgNW/PDMS electrode system. The CV diagram shown in Figure S1e, Supporting Information, exhibits the lowest first oxidation potential among these five anodically EC materials in this study, and the first oxidation state of **TPA-3DMA** could be started at a much lower potential of 0.1 V than the corresponding **TPA-3OMe** with three methoxy instead of dimethylamine units. The absorption peaks at 420 and 977 nm appeared when the applied potential was set at approximately 0.1 V, and the color change from transparent to yellow-green at 0.2 V could also be observed, as depicted in Figure 5e and Figure 6, respectively.

To fabricate an ambipolar EC system based on AgNW/PDMS hybrid electrodes, the electrochemical behavior of cathodic heptyl viologen (**HV**) as the EC material was also studied using the AgNW/PDMS hybrid electrode as the working electrode, and the CV diagram presented in Figure S1f, Supporting Information, exhibits obvious color changes from colorless to blue during reduction at −0.4 V (versus Ag/AgCl) that could also be confirmed by the absorption spectrum depicted in Figure 5f, showing an absorption peak at 606 nm at −0.4 V as reported previously on the ITO system.[21] Consequently, six different EC color forms appearing on the novel stretchable AgNW/PDMS hybrid electrodes could be obtained and are summarized
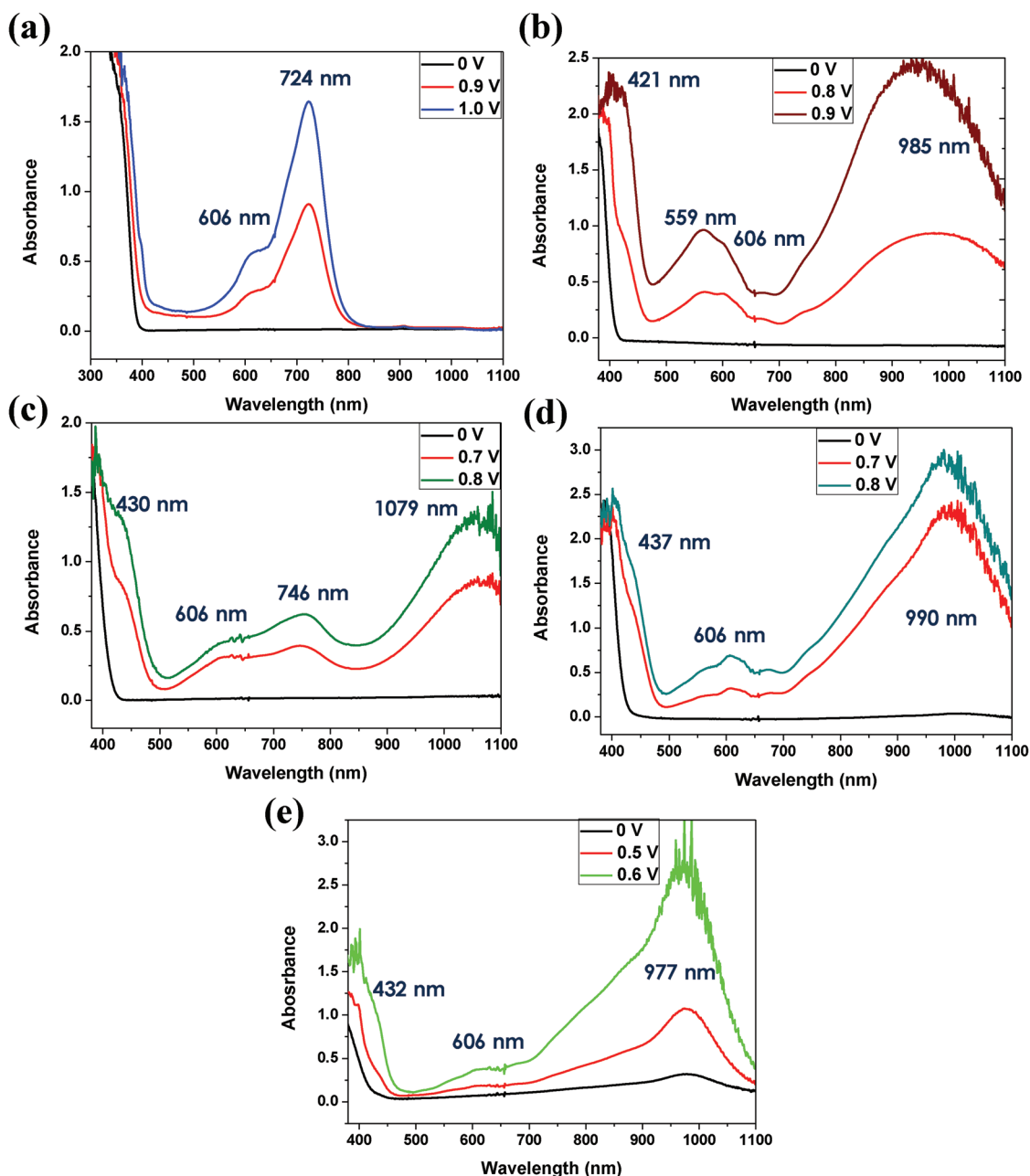
Figure 7. Absorption spectra of AgNW/PDMS ECDs (working area: 2×2 cm^2; gap thickness: 0.5 mm) with a) 3 µmole **TPA-3OMe** and 3 µmole **HV**, b) 3 µmole **TPPA** and 3 µmole **HV** in 0.2 mL of PC, c) 3 µmole **NTPPA** and 3 µmole **HV**, d) 3 µmole **SNTPPA** and 3 µmole **HV** in 0.2 mL of PC/GBL solvent (1:1 by volume), e) 3 µmole **TPA-3DMA** and 3 µmole **HV** in 0.2 mL of PC at different applied potentials.

in Figure 6. These results demonstrate that the stretchable AgNW/PDMS hybrid film as a working electrode is a feasible approach for the fabrication of ECDs and other optoelectronic applications.

2.4. Stretchable Ambipolar ECDs

Furthermore, a series of stretchable ECDs based on AgNW/PDMS hybrid electrodes were fabricated by merging the ambipolar EC materials into the devices. The detailed preparation

procedures are described in the Experimental Section. The working area, spacer thickness and sheet resistance of the devices based on AgNW/PDMS hybrid electrodes are 2×2 cm^2, 0.5 mm and 16 Ω sq^{-1}, respectively. The ambipolar EC system can provide many advantages when applied into ECDs, such as easily obtaining the merged-color appearance at a suitable applied potential, markedly enhancing the response capability, and efficiently reducing the operating voltage compared to the ECDs without an ambipolar system. Hence, five anodic TPA derivatives and cathodic HV EC materials were used to construct five distinctly ambipolar ECDs to compare their EC
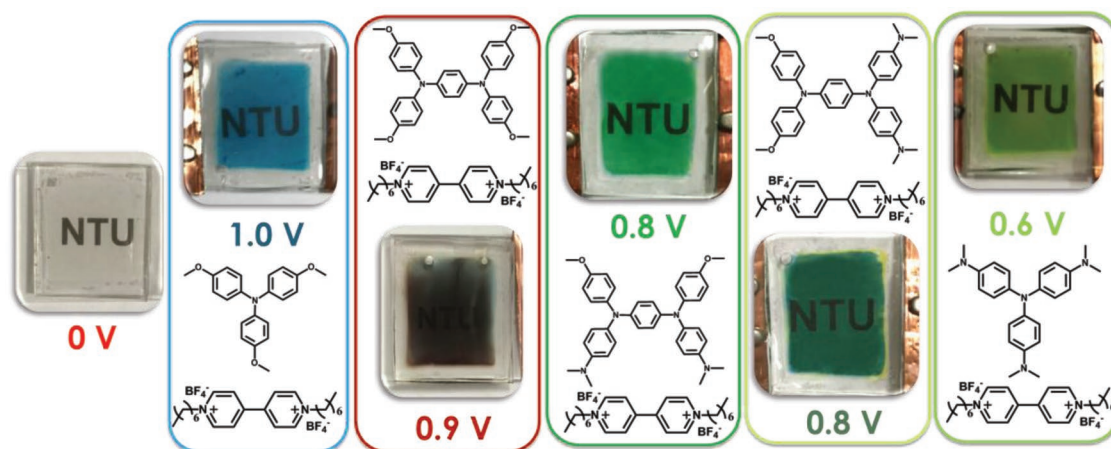
Figure 8. Summary of the EC diversity in color changes based on stretchable ambipolar ECDs.

behavior as illustrated in Figure S2, Supporting Information. The CV diagrams could furnish electrochemical information about the first redox potential of each ambipolar stretchable ECD, as labeled in Figure S3, Supporting Information, to adjust the applied potential according to these CV profiles for the subsequent spectroelectrochemical study. From the UV–vis absorption spectra of the stretchable ECDs containing **TPA-3OMe** and **HV** as illustrated in **Figure 7**a, the new absorption peaks at 606 and 724 nm appeared when the applied potential reached 0.9 V. Additionally, the color appearance of this device at the neutral state was colorless and then became blue, as shown in **Figure 8**. These characteristic absorption peaks and color forms both correspond to the merging oxidation state of **TPA-3OMe** and first reduction state of **HV**. Clearly, because the AgNW network has a less bulk-like structure that allows for more mechanical motion, the color is not influenced during the process of stretching as shown in the Supporting video. The obtained ECD exhibits elastic recovery behavior without deformation or

leakage of the EC material solution. Even after stretching and twisting for 1000 cycles, the AgNW/PDMS hybrid electrodes could retain conductivity (Figure S10, Supporting Information). This work thereby demonstrates that highly stretchable devices have mechanical stability and great potential for wearable applications.

For the devices derived from **TPPA** and **HV**, four peaks in Figure 7b could be observed at 421, 559, 606, and 985 nm when the applied potential was set at 0.8 V. These characteristic absorption peaks and color appearance also agree well with the merging the first oxidation/reduction state of **TPPA** and **HV**, respectively, and the color changes from colorless at the neutral form to deep brown in colored state as are presented in Figure 8. Afterward, the new absorption peaks of the device containing **NTPPA** and **HV** appeared at 421, 615, 746, and 1079 nm for an applied potential set at 0.7 V related to the first oxidation/reduction states of **NTPPA** and **HV**, respectively, as depicted in Figure 7c, and the color of this device in the
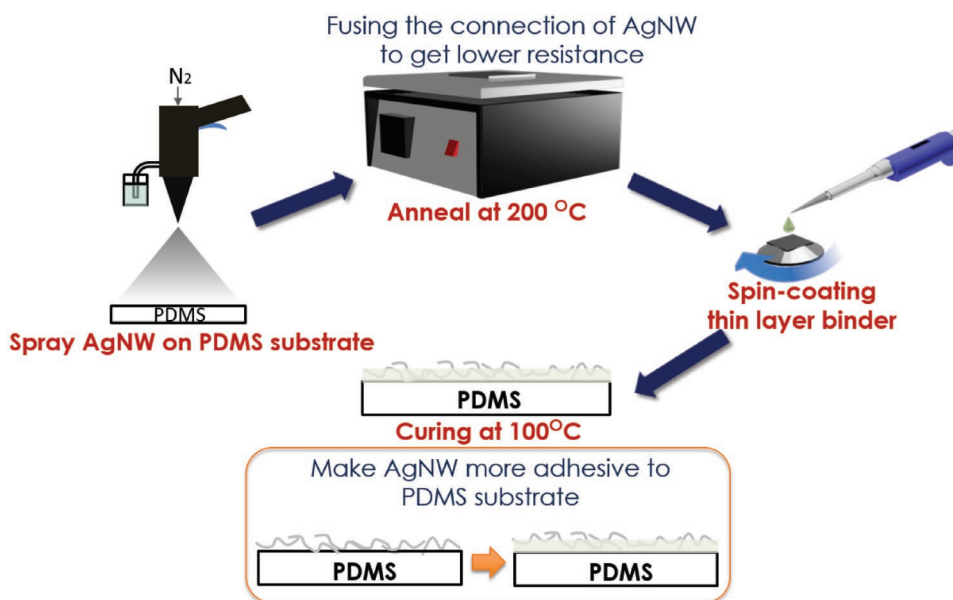
Scheme 1. Preparation route for AgNWs/PDMS hybrid electrodes.
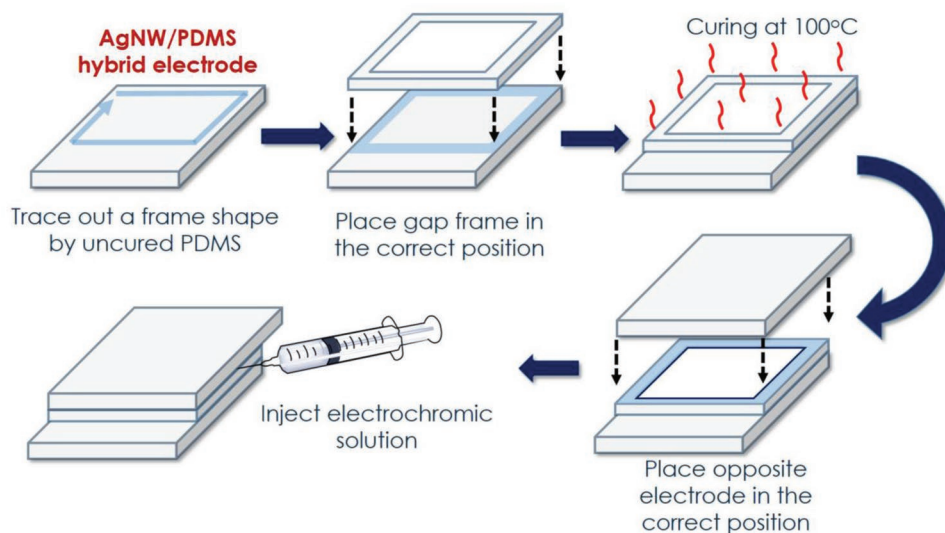
Scheme 2. Fabrication process for the stretchable ECDs.

colored state was also in line with merging the first oxidation and reduction states of **NTPPA** and **HV**, respectively, as shown in Figure 8. For the AgNW/PDMS hybrid stretchable ECD containing **SNTPPA** and **HV**, the color change from colorless to dark green also agrees well with the new absorption peaks, appearing at 437, 606, and 990 nm at 0.7 V of applied potential as depicted in Figure 7d. In addition, the stretchable ECD with color-switching behavior from colorless to yellow-green at 0.6 V could also be obtained by introducing **TPA-3DMA** and **HV** as ambipolar materials, and the related UV–vis absorption spectra and photograph are also presented in Figure 7e and Figure 8, respectively.

3. Conclusion

A facile methodology has been proposed for fabricating highly transparent and stretchable hybrid electrodes based on AgNWs with high aspect ratios. AgNW/PDMS hybrid electrodes display excellent characteristics for both electrical and optical performance, including high transmittance of 87% at 550 nm and a lower sheet resistance of 16 Ω sq^{-1}. This kind of stretchable electrode should be a potential alternative for traditional brittle electrodes for next-generation electronics, such as bendable, flexible, and stretchable displays or wearable applications.

Consequently, the technically feasible application of stretchable electrochromic devices was confirmed by introducing five TPA-based anodic and viologen-based cathodic EC materials, into AgNW/PDMS hybrid electrodes. Meanwhile, we also demonstrated that a series of highly transparent and stretchable ambipolar ECDs reveal multicolored switching from colorless to a variety of colors according to different ambipolar redox couples under suitable external applied potentials. The color-tuning behaviors of the resulting ECDs could be readily manipulated by judiciously choosing different EC materials, as summarized in Figure 8.

4. Experimental Section

Materials: Silver nitrate (99.9%, Fisher scientific), polyvinylpyrrolidone (PVP) (M_W = 1 300 000, Alfa), ethylene glycol (EG) (SHOWA), sodium chloride (NaCl) (99.5%, SHOWA), potassium bromide (KBr) (≥99%, Scharlau), *N,N*-dimethyl-*1,4*-phenylenediamine (Alfa Aesar), 10% palladium on activated carbon, hydrazine monohydrate (98+%, Alfa), *4*-bromo-*N,N*-dimethylaniline (98+%, Alfa), tris(dibenzylideneacetone) dipalladium(0) (97%, ACROS), tri-*tert*-butylphosphine (99%, STREM CHEMICAL), sodium *tert*-butoxide (98%, ACROS), and anhydrous toluene (99.8%, SIGMA-ALDRICH) were used as received without further purification. *N,N*-bis(*4*-methoxyphenyl)-1,4-phenylenediamine **(TPA-NH₂),**[22] tris(4-methoxyphenyl)amine **(TPA-3OMe),**[22] *N,N,N',N'*-tetrakis(4-methoxyphenyl)-1,4-phenylenediamine **(TPPA),**[15] *N,N'*-bis(*4*-dimethylaminophenyl)-*N,N'*-bis(4-methoxyphenyl)-*1,4*-phenylenediamine **(NTPPA),**[23] heptyl viologen tetrafluoroborate **(HV(BF₄)₂)**[22] and tetra-*n*-butylammonium tetrafluoroborate (TBABF₄)[24] were synthesized according to published methods. Cross-linked PDMS was prepared by mixing the base and the curing agent (Sylgard 184, Dow Corning) at a ratio of 10:1, and it was degassed before thermal curing.

Synthesis of AgNWs with a high aspect ratio: The AgNW sample was prepared by a one-pot polyol method, in which PVP served as the capping agent and EG served as the reductant for reducing silver nitrite into silver. At first, 0.55 g of PVP (M_W = 1 300 000) and 35 mL of pure EG were added into three necked flasks as a premixed reactant solution and stirred at room temperature for 1 h until completely dissolved under a nitrogen flow. Then, 10 mL of AgNO₃ solution (0.3 M in EG) was added into the solution at a fixed stirring rate of 260 rpm. The mixture was placed in oil bath preheated 120 °C. Then, 4 mL of NaCl (8 mM, EG solution) and 2.5 mL of KBr (4 mM, EG solution) were added into the solution, and the temperature was maintained for 4 h at 120 °C. It should be noted that the time duration of adding AgNO₃ solution, NaCl solution and KBr solution was not longer than 3 min. The color of the solution changed in the following sequence: clear orange (3 min), deep red (5 min), muddy orange (15 min), black (120 min), greenish gray (180 min), and the final white and gray color (240 min). The obtained product was then cooled at room temperature. After adding 150 mL of ethanol into the mixture, the product was then stirred for 1 day. Afterward, this mixture was centrifuged at 2600 rpm three times to separate particles from wires. Finally, the washed AgNW sample was stored in 90 mL of ethanol.

Preparation of a highly transparent AgNW/PDMS hybrid electrode: **Scheme 1** depicts the preparation route of AgNW/PDMS hybrid

**ADVANCED
SCIENCE NEWS**
www.advancedsciencenews.com

**ADVANCED
OPTICAL
MATERIALS**
www.advopticalmat.de

electrodes. The 0.01 wt% AgNWs/ethanol solution was spray-coated by an airbrush gun (nozzle diameter: 0.35 mm) onto a 3.0 × 4.0 cm^2 PDMS substrate (based on curing agent = 10:1) which was preheated at 120 °C on the hotplate. The back pressure, flow rate, and distance of spraying were adjusted as 20 psig, 20 μL s^{-1}, and 14 cm from the PDMS surface, respectively. Then, the obtained AgNW network was annealed at 200 °C for 25 min to fuse the junctions of the AgNW network, which could efficiently reduce the sheet resistance. Afterward, 10 mg of uncured PDMS solution diluted in 800 μL hexane was spin-coated onto the AgNW/PDMS substrate as a binder layer to increasing the adhesion between the AgNWs and the PDMS substrate. After curing the binder layer at 100 °C for 10 min, the AgNW/PDMS hybrid electrodes could be acquired.

Fabrication of stretchable ambipolar ECDs: The fabrication process of the stretchable ECD based on the AgNW/PDMS hybrid electrodes is described in **Scheme 2**. The AgNW/PDMS hybrid electrode was placed at the lowest layer, then a square frame (made by PDMS) 0.5 mm thick was placed onto the lowest layer electrode followed by heating on the hotplate at 100 °C for 10 min so that the electrode and frame would stick together. Then, the empty device could be obtained after the procedure was repeated with another electrode. Finally, the ECDs were successfully prepared by injecting electrochromic solution into the device with a syringe.

Supporting Information

Supporting Information is available from the Wiley Online Library or from the author.

Conflict of Interest

The authors declare no conflict of interest.

[1] Z. Wu, Z. Chen, X. Du, J. M. Logan, J. Sippel, M. Nikolou, K. Kamaras, J. R. Reynolds, D. B. Tanner, A. F. Hebard, *Science* **2004**, *305*, 1273.

[2] B. Zhou, Y. Li, G. Zheng, K. Dai, C. Liu, Y. Ma, J. Zhang, N. Wang, C. Shen, Z. Guo, *J. Mater. Chem. C* **2018**, *6*, 8360.

[3] S. Bae, H. Kim, Y. Lee, X. Xu, J. S. Park, Y. Zheng, J. Balakrishnan, T. Lei, H. R. Kim, Y. I. Song, *Nat. Nanotechnol.* **2010**, *5*, 574.

[4] Y. Sun, Y. Yin, B. T. Mayers, T. Herricks, Y. Xia, *Chem. Mater.* **2002**, *14*, 4736.

[5] D. Jiang, V. Murugadoss, Y. Wang, J. Lin, T. Ding, Z. Wang, Q. Shao, C. Wang, H. Liu, N. Lu, R. Wei, A. Subramania, Z. Guo, *Polymer Rev.* **2019**, *59*, 280.

[6] G. Zhu, X. Cui, Y. Zhang, S. Chen, M. Dong, H. Liu, Q. Shao, T. Ding, S. Wu, Z. Guo, *Polymer* **2019**, *172*, 415.

[7] Q. Hu, N. Zhou, K. Gong, H. Liu, Q. Liu, D. Sun, Q. Wang, Q. Shao, H. Liu, B. Qiu, Z. Guo, *ACS Sustainable Chem. Eng.* **2019**, *7*, 5912.

[8] a) K. Zhang, Y. Du, S. Chen, *Org. Electron.* **2015**, *26*, 380; b) X. He, R. He, A. Liu, X. Chen, Z. Zhao, S. Feng, N. Chen, M. Zhang, *J. Mater. Chem. C* **2014**, *2*, 9737; c) J. Wang, C. Yan, W. Kang, P. S. Lee, *Nanoscale* **2014**, *6*, 10734.

[9] S. K. Deb, *Appl. Opt.* **1969**, *8*, 192.

[10] V. D. Neff, *J. Electrochem. Soc.* **1978**, *125*, 886.

[11] a) K. Takada, R. Sakamoto, S. T. Yi, S. Katagiri, T. Kambe, H. Nishihara, *J. Am. Chem. Soc.* **2015**, *137*, 4681; b) J. T. S. Allan, S. Quaranta, I. I. Ebralidze, J. G. Egan, J. Poisson, N. O. Laschuk, F. Gaspari, E. B. Easton, O. V. Zenkina, *ACS Appl. Mater. Interfaces* **2017**, *9*, 40438; c) P. C. Mondal, V. Singh, M. Zharnikov, *Acc. Chem. Res.* **2017**, *50*, 2128.

[12] L. Zhao, L. Zhao, Y. Xu, T. Qiu, L. Zhi, G. Shi, *Electrochim. Acta* **2009**, *55*, 491.

[13] R. J. Mortimer, T. S. Varley, *Chem. Mater.* **2011**, *23*, 4077.

[14] a) H. J. Yen, G. S. Liou, *Polym. Chem.* **2018**, *9*, 3001; b) H. J. Yen, G. S. Liou, *Prog. Polym. Sci.* **2019**, *89*, 250.

[15] J. T. Wu, G. S. Liou, *Chem. Commun.* **2018**, *54*, 2619.

[16] a) C. Y. Yan, W. B. Kang, J. X. Wang, M. Q. Cui, X. Wang, C. Y. Foo, K. J. Chee, P. S. Lee, *ACS Nano* **2014**, *8*, 316; b) L. X. Shen, L. H. Du, S. Z. Tan, Z. G. Zang, C. X. Zhao, W. J. Mai, *Chem. Commun.* **2016**, *52*, 6296.

[17] a) C. Lee, Y. Oh, I. S. Yoon, S. H. Kim, B. K. Ju, J. M. Hong, *Sci. Rep.* **2018**, *8*, 2763; b) H. S. Liu, B. C. Pan, G. S. Liou, *Nanoscale* **2017**, *9*, 2633.

[18] V. Scardaci, R. Coull, P. E. Lyons, D. Rickard, J. N. Coleman, *Small* **2011**, *7*, 2621.

[19] W. J. Lee, M. Y. Lee, A. K. Roy, K. S. Lee, S. Y. Park, I. In, *Chem. Lett.* **2013**, *42*, 191.

[20] D. C. Huang, J. T. Wu, Y. Z. Fan, G. S. Liou, *J. Mater. Chem. C* **2017**, *5*, 9370.

[21] H. S. Liu, B. C. Pan, D. C. Huang, Y. R. Kung, C. M. Leu, G. S. Liou, *NPG Asia Mater.* **2017**, *9*, e388.

[22] a) C. W. Chang, G. S. Liou, *J. Mater. Chem.* **2008**, *18*, 5638; b) J. H. Wu, G. S. Liou, *Adv. Funct. Mater.* **2014**, *24*, 6422; c) Y. Xiao, L. Chu, Y. Sanakis, P. Liu, *J. Am. Chem. Soc.* **2009**, *131*, 9931.

[23] J. T. Wu, H. T. Lin, G. S. Liou, *ACS Appl. Mater. Interfaces* **2019**, https://doi.org/10.1021/acsami.9b00402.

[24] J. T. Wu, H. T. Lin, G. S. Liou, *J. Mater. Chem. C* **2018**, *6*, 13345.